Model for Predicting Microhardness Profiles of Steel after Nitriding

V. Horák[*], V. Hrubý and T. Mrázková

Department of Mechanical Engineering, University of Defence, Brno, Czech Republic

Abstract:

The plasma nitriding process produces a hard near-surface thin layer of the nitrided material. The thickness of the diffused layer, produced in the course of this process, is between 0.001 and 0.6 mm. The paper presents a study of influence of the nitriding temperature, pressure, and time on the steel microhardness profiles. The one-dimensional transient diffusion model is applied to a thin nitrided layer. That allows one to predict the material hardness distribution within the near-surface layer as a function of time for a modified nitrogen diffusion coefficient. The temperature and pressure dependence of the diffusion coefficient is considered. Hence, the model involves the reaction rates of nitrides formation. The solution obtained in this way is compared with experimental data for a decrease of hardness as a function of depth and time, until the core hardness is reached.

1. Introduction

The plasma nitriding is a diffusion-related treatment with the objective to increase steel surface hardness. Nitriding, as a process of chemical action of gaseous nitrogen, causes a creation of nitrides in the surface layer of material. Nitriding technology is widely used to increase the surface hardness, the fatigue resistance, as well as the corrosion protection. The thickness and composition of a surface layer are given by the course of nitrogen diffusion into a microstructure of a nitrided material and by the system of proceeding chemical reactions during the nitriding process. The nitriding process is affected by the nitriding temperature, pressure, and time.

---

[*] *Corresponding author: Department of Mechanical Engineering, University of Defence, Kounicova 65, 662 10 Brno, Czech Republic, phone: +420 973 442 616, E-mail: vladimir.horak@unob.cz*

Molecular diffusion is referred to as the penetration of molecules or atoms in a material due to a molar concentration c gradient. The unsteady-state diffusion describes Fick's second law of diffusion determining the concentration distribution during the transient diffusion in the form

$$\frac{\partial c}{\partial \tau} = D \frac{\partial^2 c}{\partial x^2},$$ (1)

where D is the diffusion coefficient expressing the ability of particles to diffuse into the material. This coefficient is a function of temperature and pressure.

The integration of this equation with respect to the initial and boundary conditions is used to determine the concentration distribution within a material. There are numerous of analytic solutions of Eq. (1) for the time-depended, one-dimensional diffusion. Such solutions are given by Crank [1] and Carslaw and Jaeger [2].

The practically important solution for the diffusion is through a semi infinite solid with constant surface concentration. Boundary conditions: for $\tau = 0$, $c = c_0$ and for $\tau > 0$, $c = c_s$ at $x = 0$ and $c = c_0$ at $x = \infty$ (see Fig. 1). Application of these boundary conditions for a plane surface yields the solution

$$\frac{c - c_0}{c_s - c_0} = 1 - \mathrm{erf}\left(\frac{x}{2\sqrt{D\tau}}\right),$$ (2)

where c is the concentration at distance x after time τ. The expression erf is the Gaussian error function [3]. The resulting concentration profiles at three different time moments τ are shown in Fig. 1.
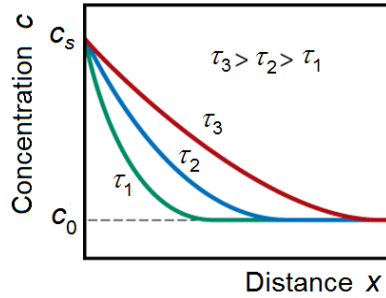

Fig. 1 Concentration profiles for unsteady-state diffusion by Eq. (2)

If we are looking for a universal representation of solution (1) in terms of elementary functions the best candidate for such an approximation is the logistic function [4] in the form

$$\frac{c - c_0}{c_s - c_0} = \frac{1}{1 + \exp\left[\dfrac{4}{\sqrt{\pi D}}(x - k\tau)\right]},$$ (3)

where the coefficient D dictates the slope of the solution and k describes the propagation of the diffusion front inside the material. Obviously, k depends not only on the physical state of the material in question but also on temperature. The resulting concentration profiles at three different time moments τ are given in Fig. 2.
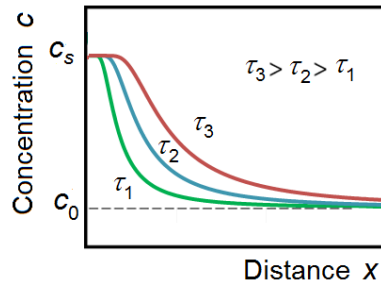
Fig. 2 Concentration profiles for unsteady-state diffusion by Eq. (3)

2. Microhardness Distribution Testing

The tested material samples were nitrided by the Rübig plasma nitriding facility for various nitriding time duration. Hardness distribution testing was performed by the Vickers's microhardness method according to DIN 50190 [5] using the automatic microindentation hardness testing system LECO LM247AT and the Amh43 software.

Results of the hardness distribution testing for 4, 9, 15, and 40 hours of nitriding process duration at the temperature 500 °C are given for the steel of the material number 32CrMoV12-10. The nitrided steel Vickers's hardness HV distribution for these four holding times of nitriding is shown in Fig. 3.

The hardness achieved on the surface HV_s decreases with the depth x until core hardness HV_0 is reached. The nitriding creates a high surface hardness and a sharp transition zone between nitrided surface and the core material. The surface hardness $HV_s = 1140$ and the core hardness $HV_0 = 520$.
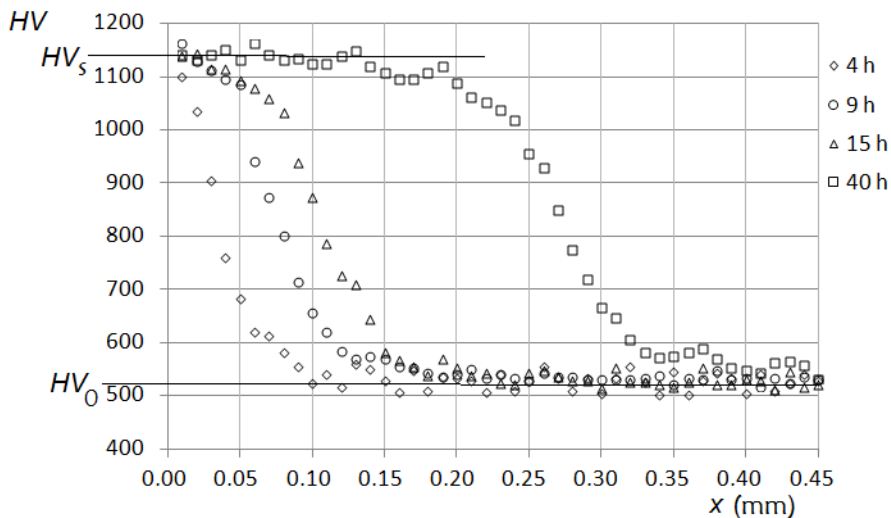

Fig. 3 Microhardness profiles for various time of nitriding, steel 32CrMoV12-10

3. Model of the Hardness Profiles for Diffusion Nitriding

The nitrided material hardness distribution should be corresponding to the concentration profile of the diffusing nitrogen. By applying the logistic function given by Eq. (3), we obtain the hardness approximation in the form

$$\frac{HV - HV_0}{HV_s - HV_0} = \frac{1}{1+\exp\left[\dfrac{4}{\sqrt{\pi D^*}}(x - k\tau)\right]} , \qquad (4)$$

where D^* is the coefficient of nitriding and k is the parameter of nitriding profile propagation.

Results of this approximation are given in Fig. 4 for $D^* = 0.003$ mm^2 and $k = 0.0072$ mm h^{-1} in comparison with the experimental data.
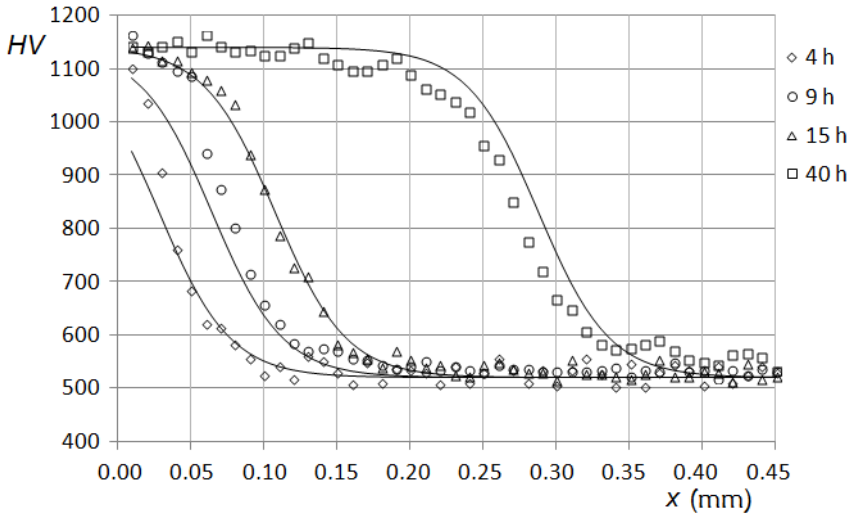

Fig. 4 Microhardness profiles approximation by equation (4) for various time of nitriding, steel 32CrMoV12-10

The logistic function (4) provides a very good approximation for various durations of nitriding as shown in Fig. 4. The coefficient of nitriding D^* takes into account for the physical properties of the material, and it is constant. The parameter of nitriding propagation k is a function of temperature. For the given material the value $k = 0.0072$ mm h^{-1} is for temperature 500 °C.

4. Combined Effect of Nitriding Time and Temperature

Results of the hardness distribution testing for various nitriding time and temperatures are shown in Fig. 5 for the steel of the material number X2CrNiMo17-12-2. The surface hardness $HV_s = 1380$ and the core hardness $HV_0 = 220$.

The logistic function (4) provides a very good approximation for various nitriding time and temperatures as shown in Fig. 5. This approximation is given for the coefficient of nitriding $D^* = 0.00007$ mm^2 and for the propagation velocities of nitriding front inside the material, which depend on temperature as:

k (450 °C) = 0.0009 mm h^{-1}
k (480 °C) = 0.0026 mm h^{-1}
k (490 °C) = 0.0033 mm h^{-1}
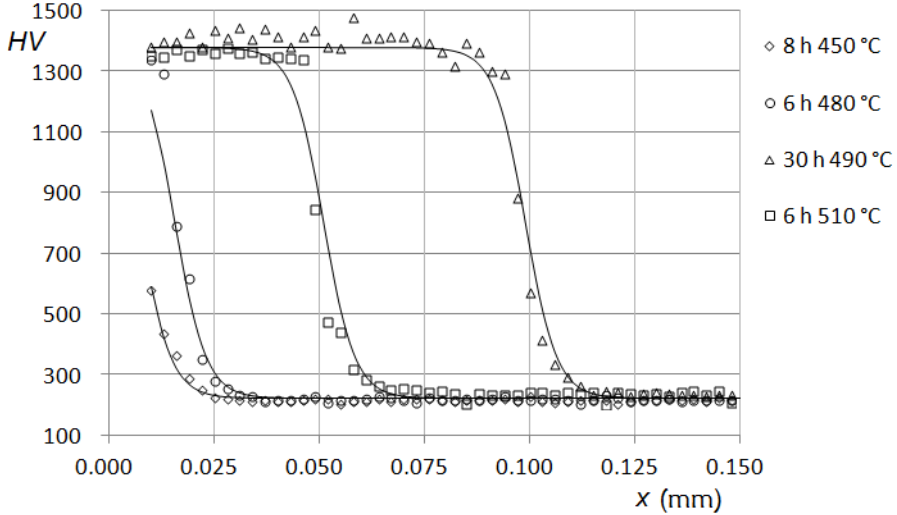k (510 °C) = 0.0085 mm h^{-1}

Fig. 5 Microhardness profiles approximation by equation (4) for varied nitriding time and temperatures, steel X2CrNiMo17-12-2

The nitriding propagation velocity k is given by the rate of chemical reactions of defunded gaseous nitrogen with the nitride-forming elements present in steel during the nitriding process. It is often found that the system must first acquire a minimum amount of energy in the course of reactions. This energy is called the activation energy E_a. Considering the general validity of van't Hoff's equation of chemical equilibrium [6], it is possible to express the dependence of the parameter of nitriding propagation velocity k on the temperature T in form known as the Arrhenius equation

$$k = k_0 \exp\left(-\frac{E_a}{R_m T}\right), \tag{5}$$

where $R_m = 8314$ J kmol^{-1} K^{-1} is the gas constant and T (K) is the absolute temperature.

Temperature has a most profound influence on the coefficients and nitriding chemical rates. The temperature dependence of nitriding propagation velocity k is related to temperature according to Eq. (5). This dependence approximated experimentally for the above outlined four temperatures is given by the pre-exponential $k_0 = 4 \times 10^{10}$ mm h^{-1} and the activation energy $E_a = 1.9 \times 10^5$ J kmol^{-1}, for the nitriding of steel X2CrNiMo17-12-2.

Since k_0, E_a, and R_m are all constants, the Arrhenius plot gives a straight line, from which the activation energy and the pre-exponential factor can both be determined [6]. Such a plot of the logarithm of the nitriding propagation k against inverse absolute temperature T is shown in Fig. 6.
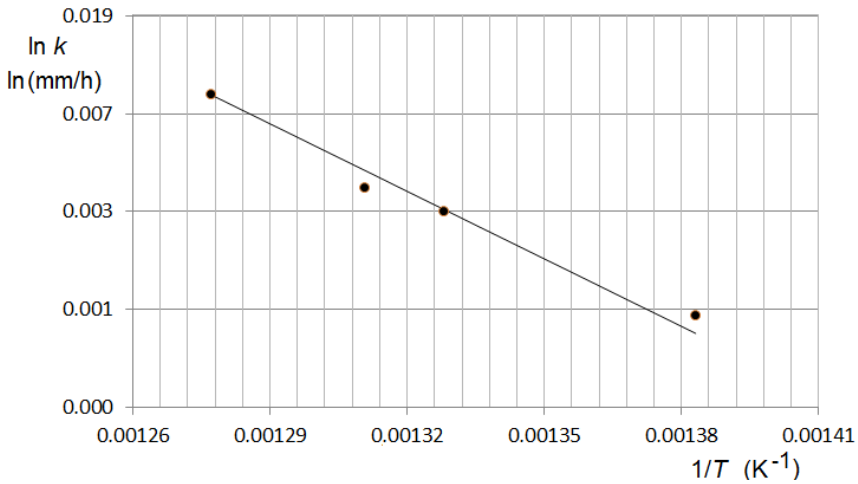
Fig. 6 Arrhenius plot of the logarithm of the nitriding propagation against inverse temperature for the nitriding of steel X2CrNiMo17-12-2

5. Effect of Nitriding Gas Pressure

The steel of material number 42CrMo4 was used to investigate the effect of the gas pressure on the nitriding response. The nitrided samples were treated for 6 hours at temperature 500 °C in the nitriding atmosphere of 25 % N_2 and 75 % H_2. The nitriding gas pressure p was changed to 400, 500, and 600 Pa.

Results of the hardness distribution testing for given pressures of nitriding gas are shown in Fig. 7. The surface hardness varies with the nitriding gas pressure and takes values HV_s = 650, 600, and 550 for pressures 400, 500, and 600 Pa. The core hardness of material HV_0 = 250.
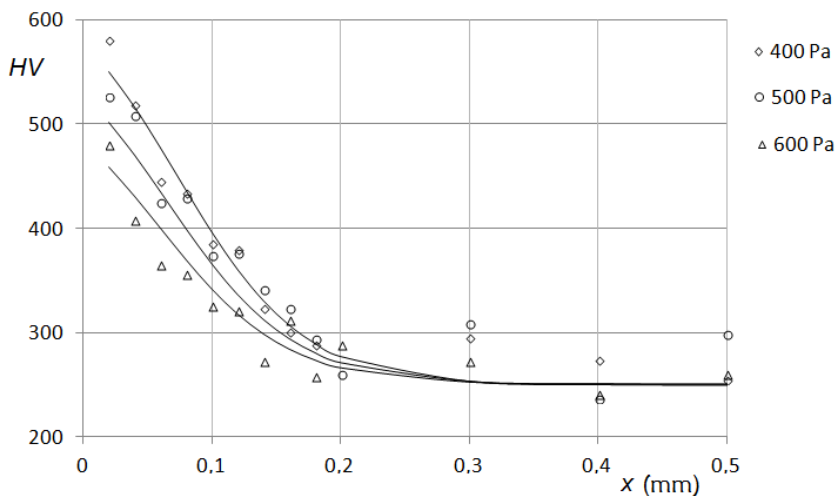

Fig. 7 Microhardness profiles approximation by equation (4) for various nitriding gas pressures, steel 42CrMo4

Approximation by the logistic function (4) corresponds very well with experimental data for various pressures as seen in Fig. 7. This approximation is given for the coefficient of nitriding $D* = 0.012$ mm^2 and for the propagation velocities of nitriding front inside the material, which depend on pressure as:

k (400 Pa) = 0.01225 mm h^{-1}

k (500 Pa) = 0.01095 mm h^{-1}

k (600 Pa) = 0.01000 mm h^{-1}

It is obvious that the effect of the nitriding gas pressure is not significant. The amount and nature of the nitride-forming elements in the steel affect the depth of nitrided layer to the extent that the penetration of nitrogen is inversely proportional to the amount of nitrogen that is precipitated (as the alloy nitrides) for a given case of nitriding process [7], i.e., the concentration of nitrogen is inversely proportional to the process pressure.

This influence can be expressed by the partial pressure p_{N2} of the nitrogen in the nitriding gas, in terms of

$$k = \frac{k_p}{\sqrt{p_{N2}}} = \frac{k_p}{\sqrt{p\,x_{N2}}}, \qquad (6)$$

where k_p is the constant of pressure effect and x_{N2} is the molar (volumetric) fraction of nitrogen, which is given by the above nitriding gas mixture composition.

A plot of the nitriding propagation velocity versus gas pressure for a given case of nitriding is shown in Fig. 8, where the constant value of pressure effect $k_p = 0.1225$ mm h^{-1} Pa$^{1/2}$ and the molar fraction of nitrogen $x_{N2} = 0.25$.
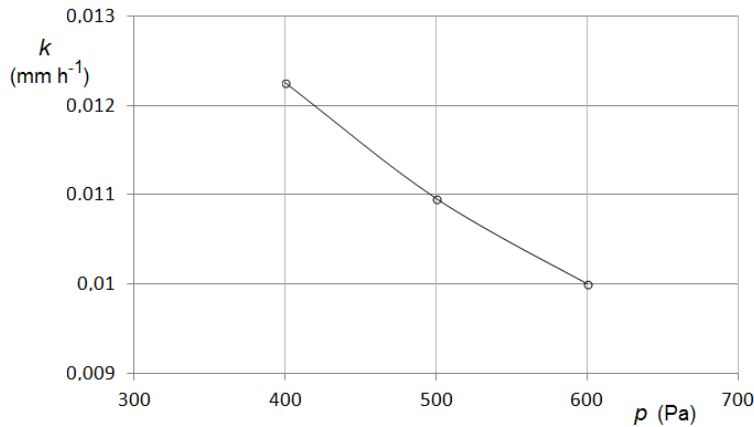

Fig. 8 Plot of the nitriding propagation velocity versus gas pressure for the nitriding of steel 42CrMo4

The influence of the pressure effect may not be unique in all nitriding cases. For instance, there were observed opposite effects of the nitriding gas pressure for the plasma nitriding of cavities of small-bored barrels [8].

6. Conclusion

In this work, a universal representation for an exact solution of the unsteady-state diffusion has been applied for the prediction of nitrided steel hardness distribution. It has been demonstrated that the logistic function is able to describe the nitriding process with high accuracy. Results of this approximation correspond very well with the experimental data for various nitriding temperatures, pressures and time durations as shown in Figs 4, 5, and 7. Moreover, only one parameter and one constant are sufficient to provide a very good fitting of experimental data.

The temperature dependence of nitriding propagation velocity was expressed by the Arrhenius equation applying the activation energy of chemical reactions. The Arrhenius plot of the logarithm of the nitriding propagation velocity versus inverse absolute temperature in Fig. 6 represents the straight line. It may be noted that the linear relationships exist for common materials [7].

The effect of the nitriding gas pressure is not significant. The nitriding propagation velocity is inversely proportional to the nitriding gas pressure as seen in Fig. 8.

The simple model developed in this study can, therefore, become a powerful tool for analyzing the process of nitriding in a wide range of applications.

Acknowledgement

References

[1]   CRANK, J. *The Mathematics of Diffusion*. Oxford: Clarendon Press, 1975.

[2]   CARSLAW, HS. and JAEGER, JC. *Conduction of Heat in Solids*. Oxford: Clarendon Press, 1959.

[3]   ABRAMOWITZ, M. and STEGUN. IA. *Handbook of Mathematical Functions*. Washington, D. C.: National Bureau of Standards, Applied Mathematics Series – 55, 1972, p. 295-300.

[4]   HORÁK, V., KULISH, V., HRUBÝ, V. and MRÁZKOVÁ, T. Model of the Hardness Prediction for the Diffusion. In. *9th Int. Conference on Mathematical Problems in Engineering, Aerospace and Sciences "ICNPAA 2012"*. New York: American Institute of Physics, Conf. Proc. 1493, 2012, p. 486-491.

[5]   DIN 50190-4: 1999. *Hardness depth of heat-treated parts – Part 4: Determination of the diffusion hardening depth and the diffusion depth.*

[6]   MOORE, WJ. *Physical Chemistry*. New York: Longman, 1998.

[7]   CALLISTER, WD. *Fundamentals of Materials Science and Engineering: An Integrated Approach.* Wiley, 2007.

[8]   POKORNÝ, Z., KADLEC, J., HRUBÝ, V., JOSKA, Z., TRAN, DQ. and BERAN, D. Plasma Nitriding of Bored Barrels. *Advances in Military Technology,* 2011, vol. 6, no. 1, p. 69-75.